Turkish Journal of Earth Sciences

Volume 31 | Number 1 Article 2

1-1-2022

Determination of recent tectonic deformations along the Tuz Gölü Fault Zone in CentralAnatolia (Turkey) with GNSS observations

CEMİL GEZGİN

SEMİH EKERCİN

İBRAHİM TİRYAKİOĞLU

BAHADIR AKTUĞ

HEDİYE ERDOĞAN

See next page for additional authors

Recommended Citation

GEZGİN, CEMİL; EKERCİN, SEMİH; TİRYAKİOĞLU, İBRAHİM; AKTUĞ, BAHADIR; ERDOĞAN, HEDİYE; GÜRBÜZ, ESRA; ORHAN, OSMAN; BİLGİLİOĞLU, SÜLEYMAN SEFA; TORUN, AHMET TARIK; GÜNDÜZ, HALİL İBRAHİM; OKTAR, OSMAN; TÜRKMEN, CEZMİ; and KAYA, EFDAL (2022) "Determination of recent tectonic deformations along the Tuz Gölü Fault Zone in CentralAnatolia (Turkey) with GNSS observations," *Turkish Journal of Earth Sciences*: Vol. 31: No. 1, Article 2. https://doi.org/10.3906/yer-2108-10

Available at: https://journals.tubitak.gov.tr/earth/vol31/iss1/2

Turkish Journal of Earth Sciences

http://journals.tubitak.gov.tr/earth/

Research Article

Turkish J Earth Sci
(2022) 31: 20-33
© TÜBİTAK
doi:10.3906/yer-2108-10

Determination of recent tectonic deformations along the Tuz Gölü Fault Zone in Central Anatolia (Turkey) with GNSS observations

Cemil GEZGİN[1,*], Semih EKERCİN[2], İbrahim TİRYAKİOĞLU[3,4], Bahadır AKTUĞ[5], Hediye ERDOĞAN[1], Esra GÜRBÜZ[1], Osman ORHAN[6], Süleyman Sefa BİLGİLİOĞLU[1], Ahmet Tarık TORUN[7], Halil İbrahim GÜNDÜZ[1], Osman OKTAR[1], Cezmi TÜRKMEN[8], Efdal KAYA[9]

[1]Department of Geomatics, Aksaray University, Aksaray, Turkey
[2]Department of Geomatics Engineering, Necmettin Erbakan University, Konya, Turkey
[3]Department of Geomatics Engineering, Afyon Kocatepe University, Afyonkarahisar, Turkey
[4]Earthquake Implementation and Research Center of Afyon Kocatepe University, Afyonkarahisar, Turkey
[5]Department of Geophysical Engineering, Ankara University, Gölbaşı, Ankara, Turkey
[6]Department of Geomatics Engineering, Mersin University, Mersin, Turkey
[7]Department of Geography, Ağrı İbrahim Çeçen University, Ağrı, Turkey
[8]Aksaray Provincial Directorate of Disaster and Emergency, Aksaray, Turkey
[9]İskenderun Vocational School, İskenderun Technical University, Hatay, Turkey

Received: 22.08.2021 • **Accepted/Published Online:** 30.11.2021 • **Final Version:** 28.01.2022

Abstract: The Tuz Gölü Fault Zone (TGFZ) is one of the most important active tectonic structures of Central Anatolia. The morphotectonic features of the TGFZ and the distribution of the epicenters of earthquakes over magnitude 5.0 show that this fault zone remains active today. In this study, the deformation of the TGFZ is determined with high sensitivity using geodetic measurements. To obtain accurate information about the deformation of the TGFZ, 24 GNSS sites and two continuously operating reference stations were constructed in the southern part of the TGFZ. Between 2018 and 2020, Global Navigation Satellite Systems (GNSS) measurements were made on this network. The data of the Turkish National Fundamental GPS Network (TNFGN) and the continuously operating reference stations-Turkey (CORS-TR) sites around the study area were also included in the study, and GNSS measurements were evaluated with the GAMIT/GLOBK software, and velocity fields of the region were determined. In addition, block modeling of the study area was calculated using the GeodSuit software. For the first time, slip rates provided by the geodetic network are established directly on the TGFZ segments, filling a significant deficiency in the literature, contributing to understanding the tectonics of the country and the region, and providing an important dataset for evaluating the degree of seismic activity of the fault zone. The slip rates obtained within the scope of this study are approximately 1.8 mm/yr strike-slip and 2 mm/yr dip-slip for the Acıpınar and Helvadere segments on that Aksaray city is built on. These results indicate that the active deformation in the TGFZ is greater than previously expressed compared to the slip rates calculated in previous studies.

Key words: Tuz Gölü Fault Zone, velocity field, block modeling, global positioning system, GPS, Central Anatolia

1. Introduction

Countries with high seismicity, such as Turkey, try to take precautionary measures to reduce the consequences of earthquakes. Many different fields of study focus on analyzing strong ground motions and understanding the plate mechanisms that cause earthquakes. In recent years, since the development of the Global Navigation Satellite Systems (GNSS) technology, the ability to determine plate mechanisms has accelerated rapidly, and many studies have been carried out to determine tectonic activities (Feigl et al., 1990; McClusky et al., 2000; Burgmann et al., 2002; Ergintav et al., 2002, Reilinger et al., 2006, Aktuğ et al., 2009; Uzel et al., 2013; Özener et al., 2010, Yavaşoğlu et al., 2011, Tatar et al., 2012; Tiryakioğlu et al., 2013, 2017; Havazlı and Özener, 2021). It is possible to obtain the latest information about a fault zone (i.e. velocity field, strain values, fault-locking depth, and shear rates) in the inter-seismic, pre-seismic, co-seismic, and post-seismic periods from evaluation of the repeated GNSS observations. These observations are repeated at certain periods using the geodetic monitoring networks established by considering the geometric structure of the fault zone (Tiryakioğlu, 2015; Doğru et al., 2019; Oktar and Erdoğan, 2018; Poyraz et al., 2019; Gezgin et al., 2020; Aktuğ et al., 2021; Eyubagil et al., 2021).

* Correspondence: cemilgezgin.jfm@gmail.com

Turkey is one of the most seismically active regions of the world (McKenzie, 1972). The neotectonic development of Turkey and its neighboring zones is closely related to the continental collision and subsequent geological processes due to the continental convergence between the Eurasian and Arabian plates (Şengör et al., 1985). Although Turkey is a country with intense seismicity, the Central Anatolian Region, in which Turkey is contained, is considered a relatively quiet region in terms of seismicity. In this region, there are secondary fault systems and fault zones that divide the Anatolian Plate into smaller blocks and contribute to the tectonic development of the entire plate (Figure 1a). Examples of these secondary fault systems and zones are the left-lateral Central Anatolian fault zone, the TGFZ, which is a normal fault zone with a right-lateral strike-slip component, the İnönü-Eskişehir fault system, and the Akşehir fault zone (Dirik and Göncüoğlu, 1996; Koçyiğit and Beyhan, 1998; Dirik, 2001; Koçyiğit, 2003; Koçyiğit and Özacar, 2003).

The Central Anatolian Region, a transition zone between other neotectonic regions in Turkey, contains active faults of different characteristics and in several directions due to the effects of the pull-apart basin from the west and the escape regime of the Anatolian Plate, which is compressed from the east (Şengör, 1980; Koçyiğit, 2003; Kürçer and Gökten, 2014a). Recent studies on the TGFZ, which is one of these active faults, show that segments of the fault zone (Acıpınar, Helvadere) around Aksaray city have the potential to generate magnitude 6.8 or greater earthquakes (Kürçer and Gökten, 2012; Emre et al., 2013; Kürçer and Gökten, 2014a). In addition, Aksaray city, which has a population of approximately 250,000 and is built on alluvial soil, was built on the Acıpınar segment of the TGFZ. Aksaray, one of the most rapidly growing cities in Turkey due to its increasing population and intense industrial potential, also hosts important national investment projects such as the Tuz Gölü Natural Gas Underground Storage Project. Therefore, determining the

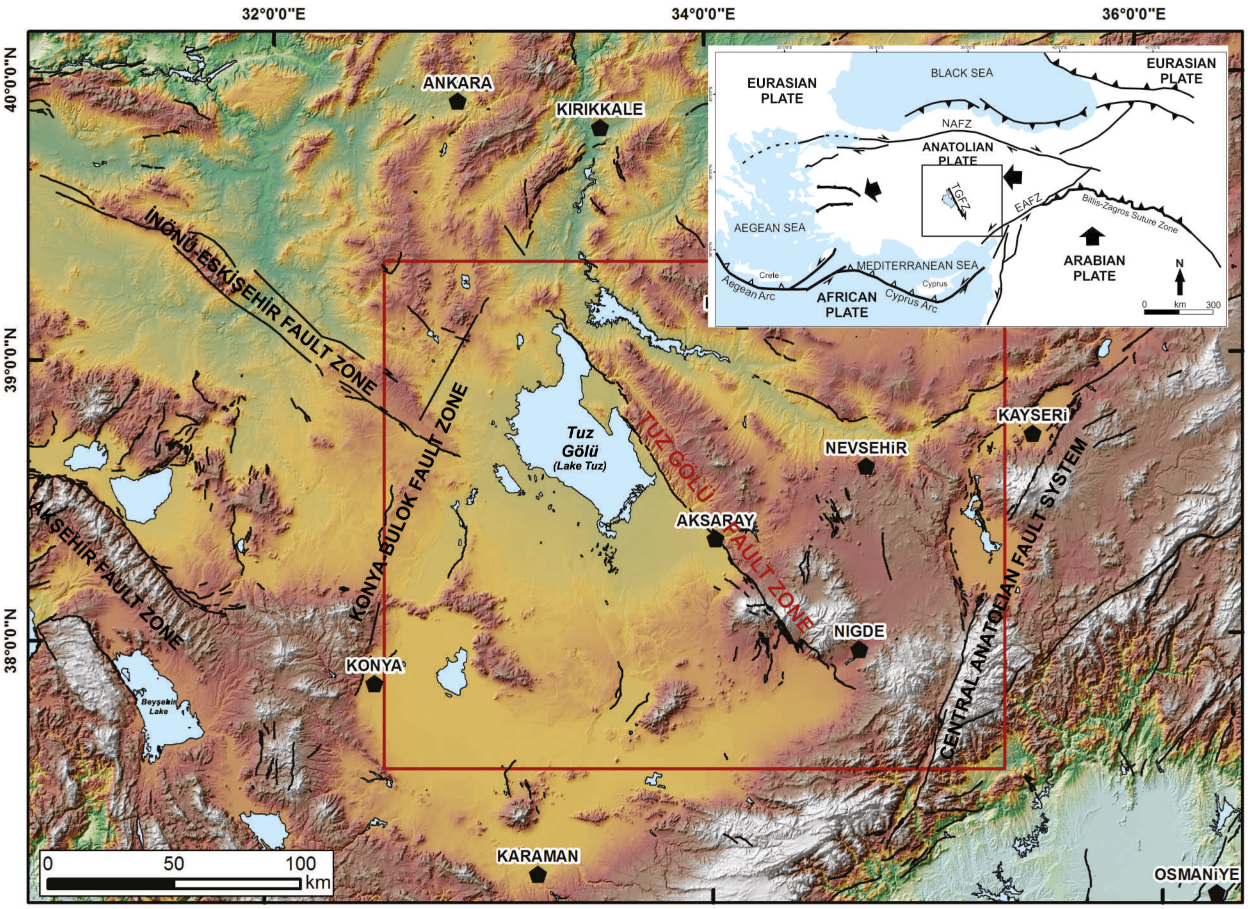

Figure 1. a) Map showing the main neotectonic elements and regions of Turkey and the location of the TGFZ (Modified from Şengör et al., 1985). Black arrows indicate GPS-derived plate rotations relative to Eurasia (Reilinger et al., 2006). **b)** Border of the study area and active faults in Central Anatolia (Dirik and Erol, 2003; Dirik, 2001; Dirik and Göncüoğlu, 1996; Göncüoğlu et al., 1996; Koçyiğit and Özacar, 2003; Özsayın and Dirik, 2007; Emre et al., 2013).

slip rate and, thus, the deformation potential of the fault zone in detail, is a necessity.

Long-term slip rates in which geological and geomorphological data are taken into account within the studies that have been conducted to determine the slip rate of the TGFZ (Çiner et al., 2011; Kürçer, 2012; Özsayın et al., 2013; Kürçer and Gökten, 2014a; Yıldırım, 2014; Öztürk et al., 2018). However, it is difficult to compare the present-day rates of faulting and the long-term geological faulting rates because of the large uncertainties of most geological estimates (Reilinger et al., 2006; Yavaşoğlu et al., 2011).

Only in the previous study, the region was investigated geodetically (Aktuğ et al., 2013), so the fault could not be evaluated based on the segments. The behaviors that led to the dissimilarities could not be determined, since the study was evaluated at the scale of Central Anatolia. The density of the GNSS sites used (30–50 km) was insufficient to determine the deformation of the TGFZ. In other words, this study does not have a large enough GNSS site density to fully determine the slip rates for the TGFZ. In other studies, Fernandez-Blanco et al. (2013) and Simao et al. (2016) have re-used the velocity vectors from Aktuğ et al. (2013), and no new measurement results related to the study area have been presented.

In this study, based on the need for a better understanding of the seismic deformation in the region, the goal is to determine the present-day slip rate and deformation area of the southern part of the TGFZ, which poses a direct threat to Aksaray, Niğde, and the surrounding provinces. For this purpose, a homogeneous geodetic network named the Tuz Gölü Tectonic GNSS Network (TUGNE) was created for the first time with this study on the southern segments of the TGFZ located in the Central Anatolia region with 24 new GNSS sites and two continuously operating reference stations (CORS). The velocity field of the region is determined using the GNSS measurements made on TUGNE and the data of TNFGN and CORS-TR stations located around the study area. Using these velocity vectors, block modeling is conducted on TGFZ using the GeodSuit software.

2. Tectonic setting

Turkey is one of the most actively deforming regions of the Alpine-Himalayan belt due to its geological location (McKenzie, 1978; Giardini et al., 2013). The main structures controlling the seismic activity of Turkey and its surroundings are the North Anatolian fault zone (NAFZ), the continental collision and the East Anatolian fault zone (EAFZ), the Aegean stress system, the sinistral Dead Sea fault zone (DSFZ), and the Aegean-Cyprus Aegean-Cyprian Arc, which is an active subduction zone (Şengör et al., 1985; Bozkurt, 2001; Aktuğ et al., 2016).

In the Central Anatolian Region of Turkey, the stress-originated basins (Tuz Gölü and Konya basins) bounded by non-parallel oblique-slip faults were defined as "plain" and this region was named the "Central Anatolian plain region" (Şengör, 1980).

Central Anatolia is a continuation of the Western Anatolian extension system, which gradually weakens toward the east. Also, the Central Anatolian Plain forms a transition zone between other neotectonic regions in our country (Şengör 1980; Dirik and Göncüoğlu, 1996; Koçyiğit and Beyhan, 1998; Dirik, 2001; Koçyiğit and Erol, 2001; Dirik and Erol, 2003; Koçyiğit and Özacar, 2003; Koçyiğit, 2005).

Because of its morphotectonic features and current micro-earthquake activity, the NW–SE-trending TGFZ, approximately 220 km long, is one of the most important active tectonic elements in Central Anatolia and has been studied by many researchers. The fault zone, which was first defined by Beekman (1966) and named the "Tuz Lake fault zone," has also been examined under the names "Tuzgölü Fault," "Koçhisar-Aksaray Fault," and "Koçhisar-Aksaray fault zone" in the studies carried out in the following years (Şengör, 1980; Uygun, 1981; Şaroğlu et al., 1987; Derman et al., 2003). Also, the TGFZ is a structure that separates the Kayseri-Sivas neotectonic region, a transtensional neotectonic regime, and the Konya-Eskişehir neotectonic region, an extensional neotectonic regime (Koçyiğit, 2000; Kürçer et al., 2012), (Figure 1a).

There are different assessments in the literature of the character of the TGFZ. According to one group of researchers, the fault has right-lateral strike slip with a thrust component (Şengör et al., 1985; Şaroğlu et al., 1987), while according to other researchers, it is a right-lateral strike-slip fault with a normal component (Beekman, 1966; Emre, 1991; Toprak and Göncüoğlu, 1993; Dirik and Göncüoğlu, 1996; Koçyiğit ve Beyhan, 1998; Çemen et al., 1999; Dirik and Erol, 2000; Toprak, 2000; Koçyiğit, 2003). According to the most recent studies carried out in the region, the fault was defined as a normal fault with a right-lateral strike-slip component (Leventoğlu, 1994; Çemen et al., 1999; Gürbüz, 2012; Özsayın et al., 2013; Kürçer and Gökten, 2014a) and according to Derman et al. (2000), it was defined as a normal fault with a left-lateral strike-slip component.

Similarly, the age of the TGFZ has been reported to be as old as the late Cretaceous (Görür and Derman, 1978; Uygun et al., 1982; Görür et al., 1984; Çemen et al., 1999; Dirik and Erol, 2000; Işık, 2009) or as young as Late Pliocene–Quaternary. (Koçyiğit, 2003; Kürçer, 2012; Gürbüz and Kazancı, 2015). Koçyiğit (2000) stated that the activation of the TGFZ post-dated the early Pliocene age, Kürçer (2012) later agreed with this assessment.

In the studies on the TGFZ, the fault zone was evaluated by the General Directorate of the Mineral Research and Exploration of Turkey (MTA) by dividing it into six segments (Duman et al., 2017). In another study by Kürçer (2012), the fault was evaluated by dividing it into 11 geometric fault segments. In this study, the segmentation chosen by the MTA was used for the calculation and visualization processes (Figure 2a).

Both the morphotectonic features of the TGFZ, which forms the northeastern border of Tuz Gölü and the distribution of the epicenters of earthquakes reaching magnitude 5 in the region indicate that this fault zone is still active today (Koçyiğit, 2003; Kürçer et al., 2012), (Figure 2b). However, studies on the deformation that may occur and the destruction it will cause in the Central Anatolia region are very limited. Kürçer et al. (2012) have determined that the Tuzgölü (2 and 3 in Figure 2a) and Akhisar-Kılıç (4 and 5 in Figure 2a) segments are the two most important structural fault segments of the TGFZ due to their length and geomorphological features. They have conducted paleoseismology studies to determine the earthquake potential of these segments. Kürçer et al. (2012) have identified four earthquakes on the Tuzgölü segment in the last 31,000 years, and the earthquake recurrence interval of this segment was 8980 years. In addition, they have determined that it has been 4010 years since the last earthquake on the segment to the present day. On the Akhisar-Kılıç segment, three earthquakes have been identified within the past 23,000 years, the earthquake recurrence period of the segment was found to be 10,390 years, and the time from the last earthquake to the present day was found to be 2340 years.

In this study, the magnitudes of the largest earthquakes that could be produced by segments close to Aksaray (3 and 4 in Figure 2a) and Niğde (5 and 6 in Figure 2a) provinces in the south of the zone were calculated. Accordingly, considering the lengths of the segments and using the equations proposed by Wells and Coppersmith (1994) for normal faults, the largest earthquakes that the Acıpınar and Helvadere segments of the TGFZ can produce are calculated as 7.2 and 6.9, respectively, and these values for the Altunhisar segment are 6.6 and 6.8. These calculations indicate that devastating damages and loss of life may occur in the surrounding provinces such as Niğde, Konya, and, in particular, in the city center of Aksaray, which is

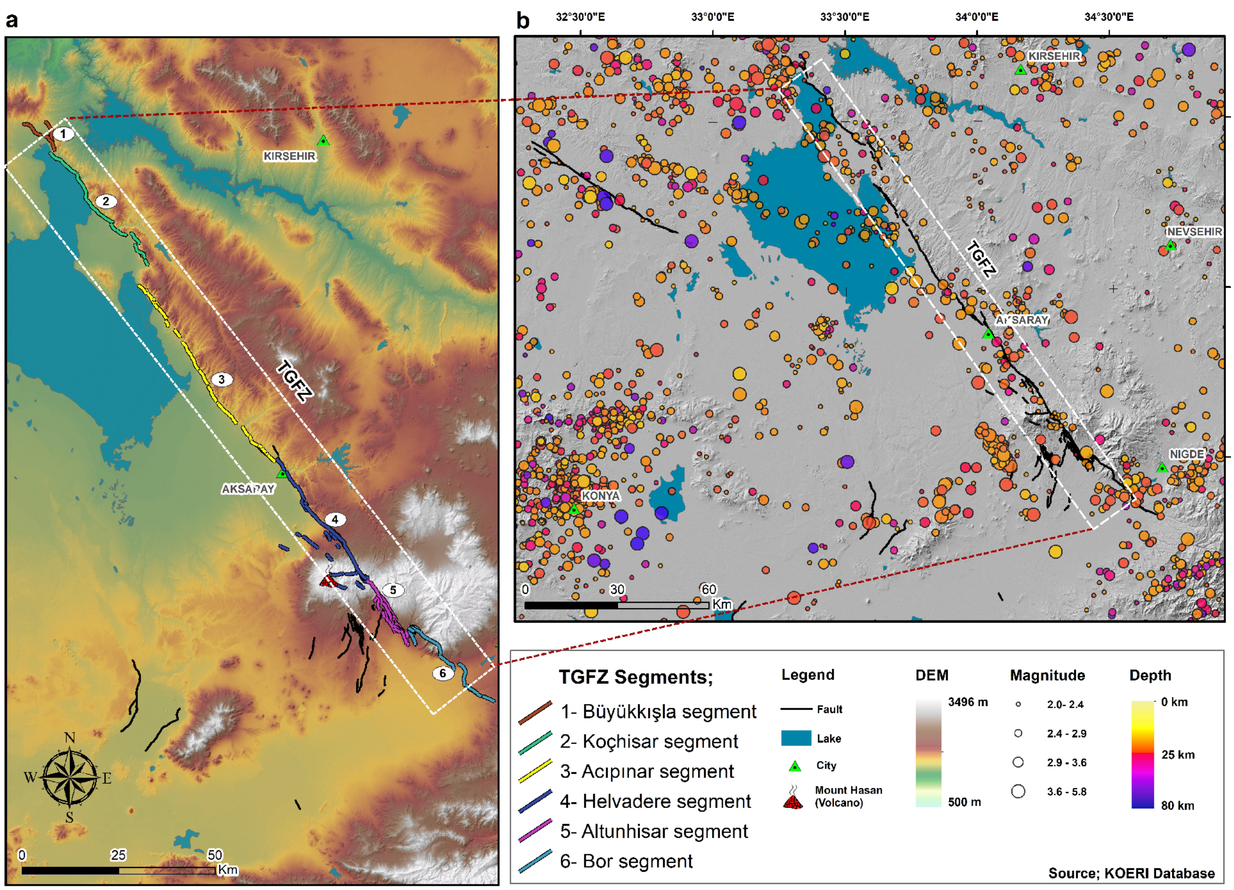

Figure 2. a) Segments of the TGFZ (Segments were taken from Duman et al., 2017) **b)** Seismicity of the TGFZ and surroundings between 1900 and June 2021 (KOERI Database). The circles represent Mw ≥ 2 earthquakes that occurred over the study area. The size of each circle represents the magnitude of the respective earthquake, while the color represents the depth.

largely built on alluvial soil. This situation necessitated creating a homogeneously distributed geodetic network with a density that can cover the fault zone in sufficient detail to detect the deformation of the TGFZ segments with high precision and monitor this network periodically.

3. GNSS observations and processing

In this study, 24 GNSS sites and 2 CORS were established in the E-NE and W-SW directions, perpendicular to the Acıpınar, Helvadere, Altunhisar, and Bor segments of the TGFZ. Thus, the Tuz Gölü Tectonic GNSS Network (TUGNE) was created for this study with a density that can characterize the southern part of the TGFZ. In addition to TUGNE, a geodetic network with a total of 51 sites with a density that can characterize the entire TGFZ was formed with 25 sites added from the CORS-TR and TNFGN networks around the study area (Figure 3).

Since the TGFZ is a right-lateral strike-slip fault, the GNSS sites were established with five cross-sectional profiles in order to detect the lateral movements of the blocks relative to each other. The number of GNSS sites in the setup profiles and the distance of these sites to the fault zone were determined depending on the depth of the seismogenic zone. A statistical evaluation of earthquake focal depths showed that earthquakes on the TGFZ occurred at an average depth of 10 km (Figure 2). The focal depths of the earthquakes occurring around Mount Hasan and Altunhisar were deeper than the average, suggesting that several earthquakes in this region might be volcanic in origin (Kürçer and Gökten, 2014a). For this reason, the GNSS sites were established at 2, 7, 15, 30, and 50 km on both sides of the fault. In addition, to monitor the tectonic movements of the region in real time, two CORS were established in the study area, approximately 5 km away and perpendicular to the fault (KRTS, CLTK in Figure 4). All of the GNSS sites on TUGNE were concrete pillars to eliminate centering errors. In this study, five campaign measurements on TUGNE, covering the period between 2018 and 2020, daily GNSS datasets between 2019 and 2020 (~22 months) of CLTK and KRTS stations, and

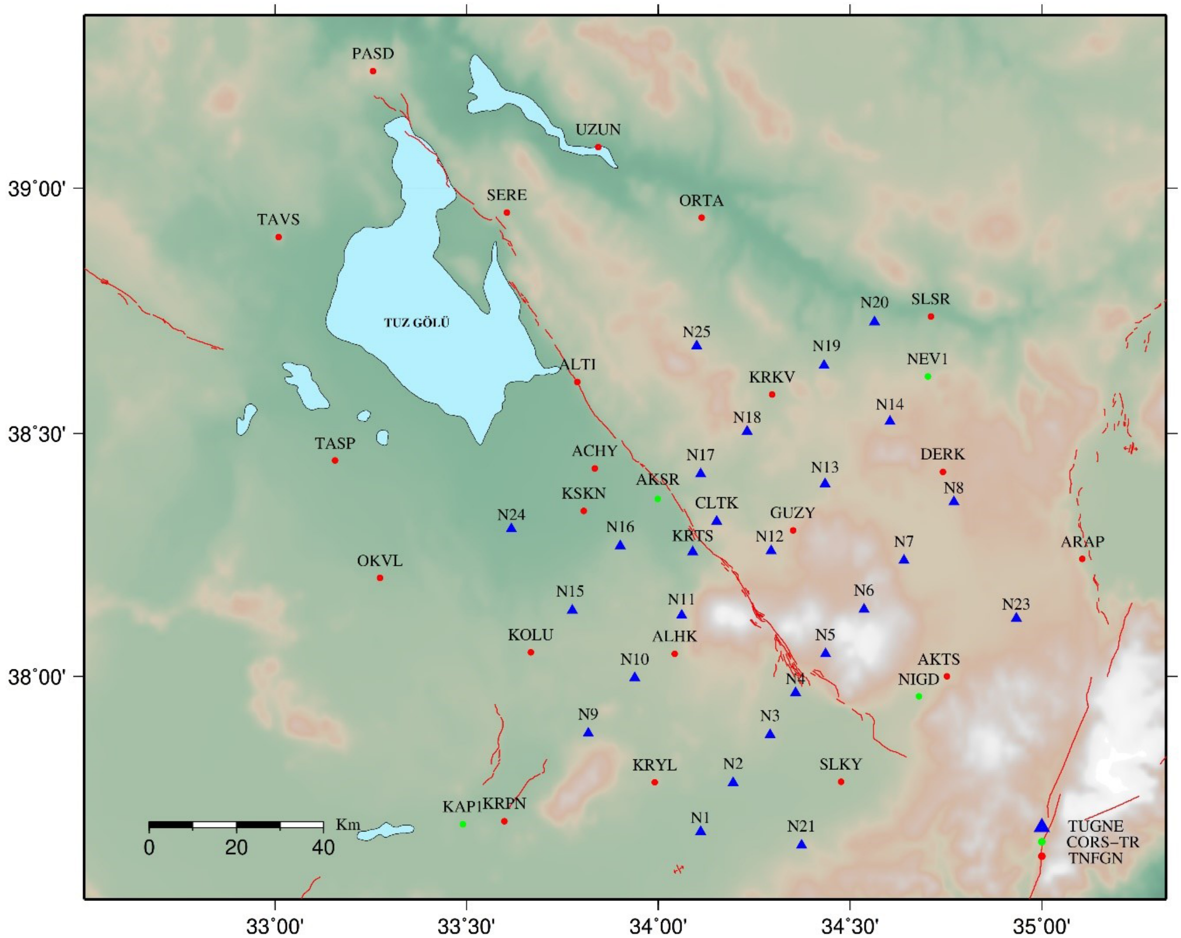

Figure 3. Map showing the Tuz Gölü Tectonic GNSS Network. TUGNE, CORS-TR, and TNFGN sites are indicated by blue triangles and green and red dots, respectively. The red lines show the active faults in the region, taken from Emre et al., 2013.

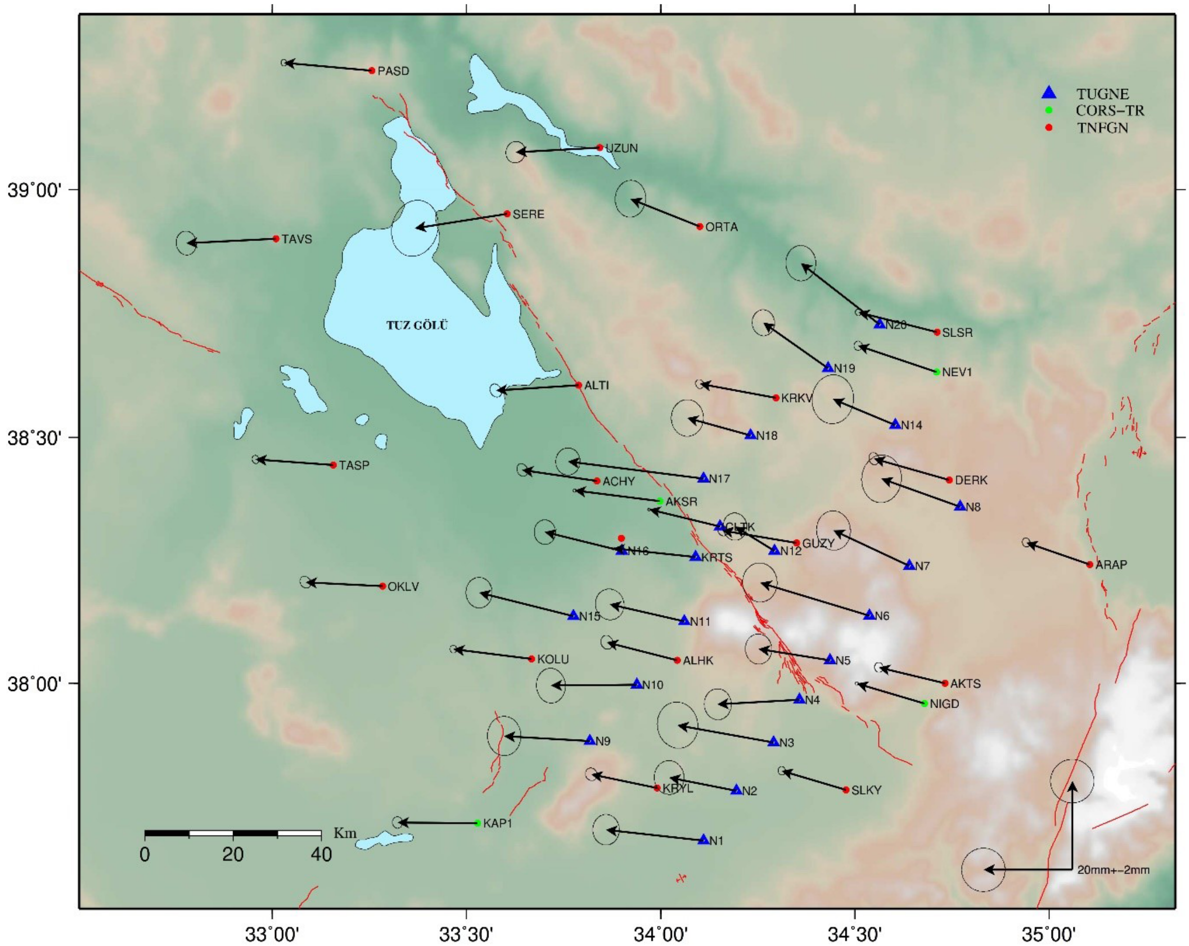

Figure 4. Horizontal velocity field of the study area in the Eurasian-fixed frame. TUGNE, CORS-TR, and TNFGN sites are indicated by blue triangles, green, and red dots, respectively. The red lines show the active faults in the region. Active faults were taken from Emre et al., 2013.

measurements obtained from CORS-TR (2015–2020) and TNFGN stations (2003–2018) were evaluated (Table 1). The GNSS results were used to obtain the velocity field of the study area and for block modeling. Campaign measurements were made in 6-month intervals in the same month of the year to minimize seasonal effects during campaigns. In measurements of the 24 GNSS campaign sites, the same GNSS receiver was used at the same station each year. The GNSS measurements were performed for 20 h over two days at all sites using 4 Topcon GR3, 6 Leica GS15, 3 Ashtech Z-Xtreme, and 7 Thales Z-Max GNSS receivers.

4. Results

4.1 GNSS velocity solution

GNSS measurements on the established network were evaluated using the GAMIT/GLOBK software package v10.71. GNSS observations were converted to RINEX format and processed in two steps. In the first step, the preliminary data that contains the position estimates is obtained with the GAMIT module. In the second step, Kalman filtering is applied to the preliminary data obtained from the GAMIT in the GLOBK module, and the solutions are obtained (King and Bock, 2000; Feigl et al., 1990). In this study, the USNO_bull_b values were used as the Earth rotation parameters (ERP). The 9-parameter Berne model, also used as a standard by SOPAC, was used for radiation pressure effects (Springer et al., 1999; Havazlı and Özener, 2021). The Scherneck model (IERS standards, 1992) was used for the ocean tide loading effect (Scherneck, 1991). The zenith delay unknowns were calculated at 2 h intervals based on the Saastamoinen a priori standard troposphere model (Saastamoinen, 1973). During the evaluation, the iono-free LC (L3) linear combination of the carrier phases L1 and L2 was used, and a height-dependent model was preferred for antenna phase centers.

Table 1. Observational spans of the sites used in the study.

Name*	**2003**	**2004**	**2006**	**2010**	**2013**	**2014**	**2015**	**2016**	**2017**	**2018**	**Name****	**2018**	**2019-1**	**2019-2**	**2020-1**	**2020-2**
ACHY			X	X			X				N.1	X	X	X		X
AKTS	X			X			X				N.2	X	X	X		X
ALHK	X			X							N.3	X	X	X	X	X
ALTI			X	X			X				N.4	X	X	X	X	X
ARAP	X					X		X			N.5	X	X	X		X
DERK			X			X		X			N.6	X	X	X	X	X
GUZY			X	X			X				N.7	X	X	X	X	X
KOLU	X			X			X				N.8	X	X	X		X
KRKV	X			X			X				N.9	X	X	X		X
KRPN				X			X				N.10	X	X	X		X
KRYL			X	X			X				N.11	X	X	X		X
KSKN			X	X							N.12	X	X	X	X	X
OKLV			X	X			X				N.14		X	X	X	X
ORTA					X			X			N.15	X	X	X		X
PASD		X			X			X			N.16	X	X	X	X	X
SERE								X	X	X	N.17	X	X	X	X	X
SLKY		X		X			X				N.18	X	X	X		X
SLSR	X					X		X			N.19	X	X	X	X	X
TASP		X				X		X			N.20	X	X	X	X	X
TAVS						X		X		X	AKSR***	X	X	X	X	X
UZUN					X			X		X	CLTK		X	X	X	X
*	These sites founded by TNFGN.										KAP1***	X	X	X	X	X
**	These sites founded by this study.										KRTS		X	X	X	X
***	These sites founded by CORS-TR.										NEV1***	X	X	X	X	X

The Eurasian plate motion was taken as the reference in accordance with the stabilization frame. In this study, 21 stations with stable time series (weighted root mean square-WRMS value of 1–2 mm for horizontal positioning) were selected for the stabilization process. As a result of the five iterative solutions performed in the evaluation, the 22 International GNSS Service (IGS) stations (ADIS, ANKR, BOR1, BUCU, CRAO, DRAG, GLSV, POLV, RAMO, TUBI, ZECK, GRAS, GRAZ, ISTA, MATE, NICO, NOT1, ONSA, POTS, SOFI, TELA, VILL) that gave the best results were used for stabilization. The post-RMS values of the velocities calculated after GLOBK stabilization were 0.30 mm/year for the Eurasian plate. The resulting GNSS velocities in the Eurasia-fixed frame are given in Table 2 and Figure 4. Some of the GNSS sites (N13, N21, N23, N24, N25, KRPN) had high RMS values due to the lack of sufficient measurements during, or destructed before, the field studies were excluded from the evaluation process.

The movement to the west and northwest directions in the Eurasian-fixed frame has been determined by examining the horizontal and vertical velocities given in Figure 4 and Table 2, and the standard deviation values of the GNSS sites vary between 1–2 mm.

4.2 Block modeling

After obtaining the velocity field of the region, block modeling was performed using the GeodSuit software and data from 45 GNSS sites to calculate the fault slip parameters. GeodSuit software is used in many studies to analyze geodetic measurements to define geodynamic parameters of tectonic events such as strain accumulations, plate motions, crustal deformations, and fault slip rates (Aktuğ et al., 2010; Tiryakioğlu et al., 2018b; Yavaşoğlu et al., 2021). The calculations were made with the block modeling module of the GeodSuit software. This module is based on Okada's (1985) theory of dislocations in Elastic Half-Space model. In this model, both in analytical and numerical methods, in order to simplify the problem, the earth's crust is assumed to be half-space instead of a whole-space where the normal stress and surface forces are zero on any of its surfaces. In this case, it is assumed that the

Table 2. Estimated velocities of the GNSS sites with 1σ uncertainties.

GNSS Site	Velocity (mm/yr)		RMS (mm/yr)		GNSS Site	Velocity (mm/yr)		RMS (mm/yr)	
	E_{vel}	N_{vel}	E_{vel}	N_{vel}		E_{vel}	N_{vel}	E_{vel}	N_{vel}
ACHY	−16.82	2.46	0.50	0.58	N7	−17.12	8.03	1.56	1.81
AKSR	−19.21	2.42	0.14	0.15	N8	−17.72	6.35	1.83	2.19
AKTS	−14.89	3.57	0.39	0.45	N9	−19.30	1.11	1.54	1.81
ALHK	−15.89	4.05	0.55	0.64	N10	−19.32	−0.16	1.33	1.60
ALTI	−18.64	−1.20	0.54	0.61	N11	−16.77	3.84	1.32	1.42
ARAP	−14.33	4.95	0.36	0.41	N12	−8.95	5.53	1.09	1.26
CLTK	−15.95	3.86	0.11	0.12	N14	−14.05	5.86	1.91	2.25
DERK	−16.96	4.81	0.47	0.56	N15	−21.25	5.32	1.21	1.41
GUZY	−16.77	2.81	0.44	0.49	N16	−17.36	4.28	0.98	1.13
KAP1	−18.01	0.16	0.46	0.53	N17	−30.52	3.86	1.12	1.25
KOLU	−17.65	2.20	0.31	0.36	N18	−14.27	3.94	1.48	1.69
KRKV	−17.17	3.18	0.36	0.42	N19	−14.62	10.31	1.03	1.20
KRTS	−18.57	1.97	0.11	0.12	N20	−17.75	13.83	1.38	1.63
KRYL	−14.79	3.08	0.54	0.58	NEV1	−17.73	5.97	0.38	0.42
TAVS	−20.18	−1.01	0.93	1.10	UZUN	−18.94	−1.04	0.89	0.99
PASD	−19.80	1.78	0.26	0.31	KSKN	−17.66	3.16	0.86	1.05
N1	−22.00	2.43	1.22	1.41	TASP	−17.52	1.27	0.32	0.38
N2	−15.14	2.98	1.37	1.56	NIGD	−15.24	4.51	0.15	0.16
N3	−21.63	3.87	1.87	2.13	OKLV	−17.34	0.86	0.50	0.55
N4	−18.45	−1.03	1.24	1.43	ORTA	−15.64	6.22	1.40	1.70
N5	−16.11	2.56	1.22	1.39	SERE	−20.77	−3.26	2.15	2.58
N6	−24.63	7.44	1.59	1.80	SLKY	−14.49	4.30	0.34	0.39
					SLSR	−17.72	4.47	0.27	0.31

surface forces and stress values of one of the blocks are constant in block modeling. Accordingly, the analytical equations used in this study for strike-slip and dip-slip in a rectangular area (fault plane) are given below.

For strike slip;

$$u_x = -\frac{U_1}{2\pi}\left[\frac{\xi q}{R(R+\eta)} + \tan^{-1}\frac{\xi\eta}{qR} + I_1 \sin\delta\right] \tag{4.1}$$

$$u_y = -\frac{U_1}{2\pi}\left[\frac{y' q}{R(R+\eta)} + \frac{q\cos\delta}{R+\eta} + I_2 \sin\delta\right] \tag{4.2}$$

$$u_z = -\frac{U_1}{2\pi}\left[\frac{d' q}{R(R+\eta)} + \frac{q\sin\delta}{R+\eta} + I_4 \sin\delta\right] \tag{4.3}$$

For dip-slip;

$$u_x = -\frac{U_2}{2\pi}\left[\frac{q}{R} + I_3 \sin\delta \, . \cos\delta\right] \tag{4.4}$$

$$u_y = -\frac{U_2}{2\pi}\left[\frac{y' q}{R(R+x')} + \cos\delta \, . \tan^{-1}\frac{x'\eta}{R+\eta} - I_1 \sin\delta \, . \cos\delta\right] \tag{4.5}$$

$$u_z = -\frac{U_2}{2\pi}\left[\frac{y' q}{R(R+\xi)} + \sin\delta \, . \tan^{-1}\frac{\xi\eta}{qR} - I_5 \sin\delta \, . \cos\delta\right] \tag{4.6}$$

In the equations given above (Eq. 4.1-4.6), U_i are slip vector components, δ is dip angle, y' and d' denotes the center of the coordinate system of the fault plane and its coordinates in a coordinate system parallel to the fault plane, ξ, η and q represents the coordinates on the fault plane coordinate system of the fault plane origin, R is the distance of the fault starting point to the origin, u_i (i: x, y, z) represents the fault direction, dip angle and displacements perpendicular to the fault plane, respectively.

In the block modeling, the block boundaries are determined using the fault geometries defined in the region first. The block boundaries are defined as the two main sections of the TGFZ. The first block is the NE block of the TGFZ (Block 1). The second block is the SW block of the TGFZ (Block 2). In the block definition, the faults were defined as SW dipping, the rigidity of the Earth's crust was 30 GPa (Aydan, 2000; Tiryakioğlu et al., 2018a). The average earthquake depth in the region is determined to be 10 km (Kürçer, 2012; KOERI Database), and therefore, we assumed a uniform locking depth of 10 km for TGFZ in our modeling process. We used 68°, 70°, and 78° dip angles in the three-segment model and 68°, 70°, 74°, and 81° in the four-segment model, from north to south, respectively. The dip angles were calculated from the fault slip data reported in Kürçer and Gökten (2014a). In block modeling, two different models were created to examine the changes in the three-segment and four-segment formation of the two-block fault, and the slip rates were separately calculated for each of them. In the three-segment model, segments 1, 2, and 3 are defined together as the first segment, segment 4 is the second segment, and segments 5 and 6 as taken together as the third segment (Figure 5). In the four-segment model, unlike the three-segment model, segments 5 and 6 are evaluated separately (Figure 6). Block modeling was performed according to these block boundaries and segmentation, and strike-slips, dip-slips, and residual velocities were obtained. On the other hand, weighted root mean square (WRMS) and normalized root mean square (NRMS) values were determined for the block models using the formulations given in Equations 4.7 and 4.8.

$$nrms = \sqrt{\frac{\sum \left(\frac{r}{\sigma}\right)^2}{n-1}} \tag{4.7}$$

$$wrms = \sqrt{\frac{n}{n-2} \frac{\sum \left(\frac{r}{\sigma}\right)^2}{\sum \left(\frac{1}{\sigma}\right)^2}} \tag{4.8}$$

In the equations given above (Eq. 4.7–4.8), r is the residual, σ is the residual velocity formal error, and n is the number of observations. The NRMS identifies as the unitless marker of how good the data are fit and should

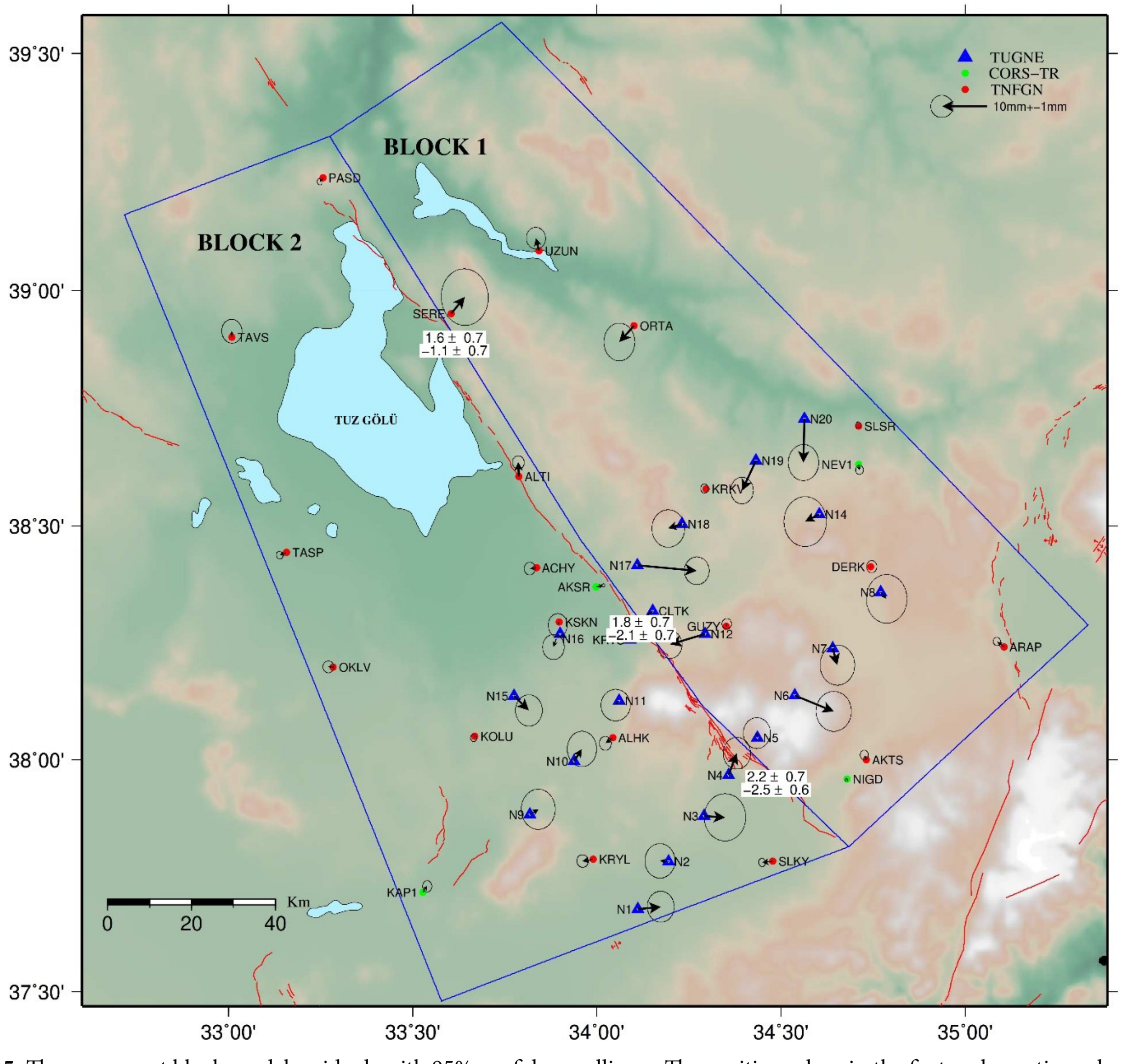

Figure 5. Three-segment block model residuals with 95% confidence ellipses. The positive values in the first and negative values in the second row correspond to right-lateral and normal slips, respectively.

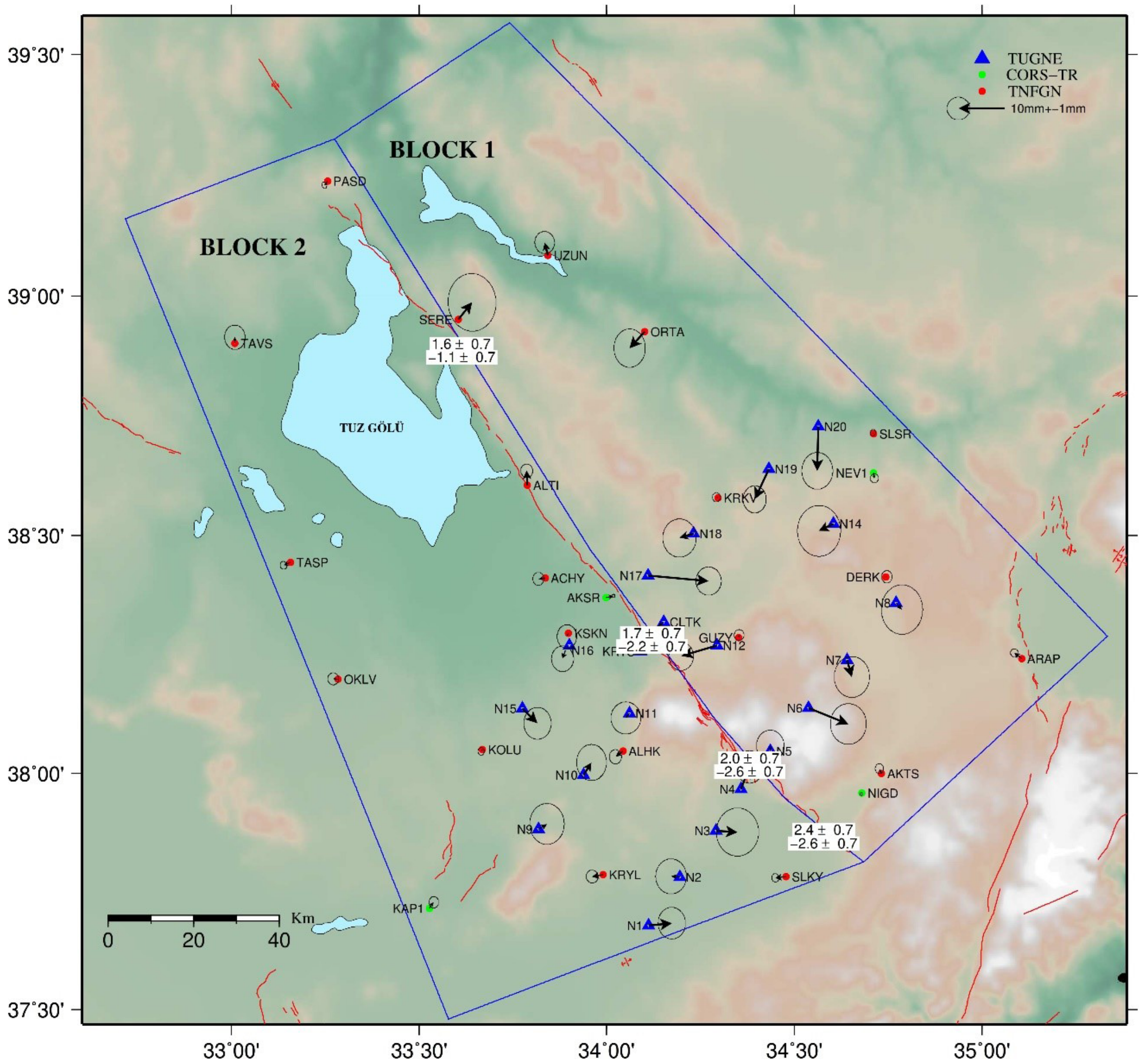

Figure 6. Four-segment block model residuals with 95% confidence ellipses. The positive values in the first and negative values in the second rows correspond to right-lateral and normal slips, respectively.

be near unity while the WRMS gives a measure of the a posteriori weighted scatter in the fits and has units of the measurement kind. (McCaffrey, 2005).

In Figure 4, where the TGFZ is evaluated as three segments, 1.6 ± 0.7 mm/yr strike-slip and −1.1 ± 0.7 mm/yr dip-slip rates are obtained in the northern part of the TGFZ, which includes the Büyükkışla, Koçhisar, and Acıpınar segments. The slip rates calculated for the central part of the TGFZ, which includes the Helvadere segment, are 1.8 ± 0.7 mm/yr and −2.1 ± 0.7 mm/yr. For the southern part of the TGFZ that represents the Altunhisar and Bor segments as a whole, the values obtained are 2.2 ± 0.7 mm/yr and −2.5 ± 0.6 mm/yr.

The four-segment model, in which Altunhisar and Bor segments are evaluated separately, differs from the three-segment model and is shown in Figure 6. In this model, the slip rates obtained were 2.0 ± 0.7 mm/yr strike-slip and −2.6 ± 0.7 mm/yr dip-slip; and 2.4 ± 0.7 mm/yr strike-slip and −2.6 ± 0.7 mm/yr dip-slip, for the Altunhisar and Bor segments, respectively. When the two models (Figure 5 and Figure 6) are compared, the obtained slip rates are approximately equal, and these two models are compatible with each other. When Figures 5 and 6 are examined, it is seen that slip rate values are significant with 95% confidence ellipses. Normalized RMS = 2.38 mm and weighted RMS = 1.00 mm were computed for the both three-segment and four-segment models. However, it is thought that the block model residuals will reduce as the number of GNSS measurements made in the established geodetic network increases.

5. Discussion and conclusion

This study explored the current velocity field and slip rates of the TGFZ, a major tectonic structure in the Central Anatolia region. For this purpose, a region-specific GNSS network (TUGNE), composed of campaign observation sites and continuously operating stations, was built to clarify the kinematic characteristics of the tectonically active TGFZ and also contribute to the understanding of tectonics on regional and country scales. First, due to the lack of previous GNSS campaign datasets in the region, new GNSS observations were conducted across the TGFZ and surroundings to determine recent tectonic deformations. Therefore, GNSS observations performed in 2020 on TUGNE, which was the fifth campaign after 2018 and 2019, have major value for comprehending the recent kinematics of the TGFZ and the Central Anatolian Region. In addition to the new dataset acquired in 2020, two continuously operating GNSS stations were merged into our regional network to densify the observation sites spatially and temporally. The new campaign dataset and the data from the continuously operating GNSS stations provided from this study are unique datasets that were not available previously.

These new datasets have allowed the precise estimation of velocity values for the TGFZ and its surroundings. The final estimated velocity values for the GNSS sites on and around the TGFZ reach 20 mm/yr in the horizontal direction. The GNSS velocity values provided from this study are compatible with earlier studies (Reilinger et al., 2006; Aktuğ et al., 2013; Simao et al., 2016).

Many studies have been conducted using different methods to calculate slip rates in the region. The geological vertical slip rates of the TGFZ offered in earlier studies are 2–4 mm/year for the last 23,000 years (Çiner et al., 2011), 0.05 mm/year based on deformed ignimbrites (Kürçer and Gökten, 2012), 0.08 and 0.13 mm/year based on a displaced Late Miocene–Early Pliocene limestone horizon (Özsayın et al., 2013), and 0.05 and 0.5 mm/year from geomorphic analyses (Yıldırım, 2014). It is hard to compare the recent faulting rates with the long-term geological rates due to the uncertainties of the geological estimates (Reilinger et al., 2006). However, the published geological vertical slip rates are consistent with the slip rates derived from GNSS in this study.

The GNSS-derived slip rates of the TGFZ obtained from this study in a three-segment model are 1.6 ± 0.7 mm/yr and −1.1 ± 0.7 mm/yr (segments 1, 2 and 3), 1.8 ± 0.7 mm/yr and -2.1 ± 0.7 mm/yr (segment 4), 2.2 ± 0.7 mm/yr and −2.5 ± 0.6 mm/yr (segment 5 and 6) from north to south. The positive value in the first slip rate indicates right-lateral movement and the negative value in the second slip rate indicates normal slip. In the four-segment model, where segments 5 and 6 are evaluated separately, the slip rates of segment 5 were obtained as 2.0 ± 0.7 mm/yr and −2.6 ± 0.7 mm/yr. Slip rates of the segment 6 are calculated as 2.4 ± 0.7 mm/yr and −2.6 ± 0.7 mm/yr.

Although there is no detailed block model study using GNSS velocities in the region, a block model including the study area was published in Aktuğ et al. (2013). The GNSS-derived slip rates of the TGFZ determined by Aktuğ et al. (2013) are 4.7 ± 0.1 mm/year right-lateral slip and 1.2 ± 0.1 mm/year normal slip, based on a block residual model. Since the study was evaluated at the scale of the entire Central Anatolian Region, fewer GNSS sites were used to determine the slip rate of TGFZ compared to this study. Even so, the block model results obtained from this study and Aktuğ et al. (2013) are consistent with each other. However, only the GNSS site distribution used for the first time in this study is dense enough to correctly represent the southern part of TGFZ. In the paleoseismological studies (Kürçer et al., 2012; Kürçer and Gökten, 2014b) carried out in the region, the time elapsed from the last earthquake to the present was found to be 4010 years for the Tuz Gölü segment and 2340 years for the Akhisar-Kılıç segment. In addition, the annual slip rate of the TGFZ was calculated as 0.040 – 0.053 mm (average 0.046 mm) in these studies. Contrary to the slip rates obtained in paleoseismological studies, the geodetic slip rates obtained within the scope of this study indicate that the active deformation in the zone is actually higher than stated.

Acknowledgment

This research was supported by the Scientific and Technological Research Council of Turkey (TUBITAK, Project Number: 118Y068) and Disaster and Emergency Management Presidency of Turkey - AFAD (UDAP, Project Number UDAP-Ç-18-01). The authors would like to thank Asuman Akşit for her contributions to the UDAP project.

References

Aktug B, Nocquet JM, Cingöz A, Parsons B, Erkan Y et al. (2009). Deformation of western Turkey from a combination of permanent and campaign GPS data: Limits to block-like behavior. Journal of Geophysical Research 114 (B10). doi: 10.1029/2008jb006000

Aktug B, Kaypak B, Çelik RN (2010). Source parameters of 03 February 2002 Çay earthquake, Mw 6.6 and aftershocks from GPS data, southwestern Turkey. Journal of Seismology 14: 445-456.

Aktug B, Parmaksız E, Kurt M, Lenk O, Kılıçoglu A et al. (2013). Deformation of Central Anatolia: GPS implications. Journal of Geodynamics 67: 78-96.

Aktug B, Özener H, Doğru A, Sabuncu A, Turgut B et al. (2016). Slip rates and seismic potential on the east anatolian fault system using an improved GPS velocity field. Journal of Geodynamics 94–95: 1–12.

Aktug B, Tiryakioğlu İ, Sözbilir H, Özener H, Özkaymak Ç et al. (2021). GPS Derived Finite Source Mechanism of the 30 October 2020 Samos Earthquake, Mw=6.9 in Aegean extensional region. Turkish Journal of Earth Sciences 30: 718-737. doi: 10.3906/yer-2101-18

Aydan Ö (2000). A new stress inference method for the stress state of Earth's crust and its application. Yerbilimleri 22: 223-236.

Beekman PH (1966). The pliocene and quaternary volcanism in the Hasan Dağ-melendiz dağ region. MTA Bulletin 66: 90-105.

Bozkurt E (2001). Neotectonics of Turkey - A synthesis. Geodinamica Acta 14 (1-3): 3-30.

Burgmann R, Ayhan ME, Fielding EJ, Wright TJ, McClusky S et al. (2002). Deformation during the 12 November 1999 Düzce, Turkey Earthquake, from GPS and InSAR Data. Bulletin of the Seismological Society of America 92 (1): 161-171.

Çemen İ, Göncüoğlu MC, Dirik K (1999). Structural evolution of the Tuzgölü basin in Central Anatolia, Turkey. Journal of Geologys 107: 693-706.

Çiner A, Aydar E, Dirik K, Rojay B, Özsayın E, Ersoy O, Çubukçu E, Kutluay A, Yıldırım, C (2011). Vertical Anatolian Movement Project (VAMP), TÜBİTAK Project No: 107Y333

Derman AS, Rojay B, Güney H, Yıldız M (2000). Koçhisar-Aksaray fay zonu'nun evrimi hakkında yeni veriler, Haymana-Tuzgölü-Ulukışla basenlerinin uygulamalı çalışması. Bildiri Özetleri, 1, Aksaray (in Turkish).

Derman AS, Rojay B, Güney H, Yıldız M (2003). Koçhisar-Aksaray fay zonu'nun evrimi hakkında yeni veriler. Türkiye Petrol Jeologları Derneği Haymana-Tuzgölü-Ulukışla Basenleri Uygulamalı Çalışma-2001 (in Turkish).

Dirik K, Erol O (2000). Tuzgölü ve civarının tektonomorfolojik evrimi Orta Anadolu, Türkiye Haymana-Tuzgölü-Ulukışla Basenleri Uygulamalı Çalışma (Workshop). TPJD Bülteni, Özel sayı 5 (in Turkish).

Dirik K, Erol O (2003). Tuzgölü ve civarının tektonomorfolojik evrimi, Orta Anadolu-Türkiye. Türkiye Petrol Jeologları Derneği Özel Sayı 5: 27-46 (in Turkish).

Dirik K, Göncüoğlu MC (1996). Neotectonic characteristics of Central Anatolia. International Geology Review 38: 807-817.

Dirik K (2001). Neotectonic evolution of the northwestward arched segment of the Central Anatolian fault zone, Central Anatolia, Turkey. Geodinamica Acta 14: 147-158.

Doğru A, Aktuğ B, Bulut F, Özener H (2019). GPS-derived source parameters of the 2014 North Aegean earthquake (Mw 6.9). Turkish Journal of Earth Sciences 28 (5): 661-670.

Duman TY, Emre Ö, Selim Özalp S, Çan T, Olgun Ş et al. (2017). Türkiye ve yakın çevresindeki diri faylar ve özellikleri. Türkiye Sismotektonik Haritası Açıklama Kitabı (Ed. T.Y. Duman). Maden Tetkik ve Arama Genel Müdürlüğü Özel Yayınlar Serisi-34, 12 s. Ankara-Türkiye.

Eyubagil E, Solak H, Kayak U, Tiryakioglu I, Sozbilir H et al. (2021). Present day strike-slip deformation within the southern part of the Izmir-Balikesir Transfer Zone based on GNSS data and implications for seismic hazard assessment in western Anatolia. Turkish Journal of Earth Sciences 30 (2): 143-160.

Emre Ö (1991). Hasandağı-Keçiboyduran Dağı Volkanizmasının Jeomorfolojisi. PhD, İstanbul University, İstanbul, Turkey (in Turkish).

Emre Ö, Duman TY, Özalp S, Elmacı H, Olgun Ş et al. (2013). Açıklamalı Türkiye Diri Fay Haritası, Ölçek 1:1.250.000. Maden Tetkik ve Arama Genel Müdürlüğü, Özel Yayın Serisi, 30, Ankara (in Turkish).

Ergintav S, Bürgmann R, McClusky S, Çakmak R, Reilinger RE et al. (2002). Postseismic deformation near the İzmit Earthquake (08/17/1999, M =7.5) rupture zone. Bulletin of the Seismological Society of America 92 (1): 194-207.

Feigl KL, King RW, Jordan TH (1990). Geodetic measurement of tectonic deformation in the santa maria fold and thrust belt, California. Journal of Geophysical Research 95 (B3): 2679-2699.

Fernandez-Blanco D, Bertotti G, Çiner A (2013). Cenozoic tectonics of the Tuz Gölü Basin (Central Anatolia Plateau, Turkey). Turkish Journal of Earth Sciences 22 (5): 715-738.

Fowler CMR (1990). The solid earth-An introduction to Global Geophysics, Cambridge University press, Cambridge

GeodSuit (2017). GeodSuit deformation nodule user manual. Ankara, Turkey.

Gezgin C, Tiryakioğlu İ, Ekercin S, Gürbüz E (2020). Monitoring of tectonic movements of southern part of the Tuz Gölü Fault Zone (TGFZ) with GNSS Observations. Afyon Kocatepe Üniversitesi Fen ve Mühendislik Bilimleri Dergisi 20 (3): 456-464 (in Turkish with English abstract).

Giardini D, Woessner J, Danciu L, Crowley H, Cotton F et al. (2013). European Seismic Hazard Map for Peak Ground Acceleation, 10% Exceedance Probabilities in 50 years.

Görür N, Derman AS (1978). Tuzgölü-Haymana havzasının stratigrafik ve tektonik analizi, TPAO Rapor, 1514 (in Turkish).

Görür N, Oktay FY, Seymen I, Şengör AMC (1984). Palaeotectonic evolution of the Tuzgölü basin complex, Central Turkey: sedimentary record of a Neo-Tethyan closure. Geological Society, London, Special Publications 17 (1): 467-482.

Gürbüz A, Kazancı N (2015). Genetic framework of Neogene–Quaternary basin closure process in central Turkey. Lithosphere 7 (4): 421-426.

Gürbüz A (2012). Tuz Gölü Havzası'nın Pliyo- Kuvaterner'deki Tektono-sedimanter evrimi. PhD, Ankara Üniversitesi, Fen Bilimleri Enstitüsü, Ankara, Turkey (in Turkish).

Havazlı E, Özener H (2021). Investigation of strain accumulation along Tuzla fault – western Turkey. Turkish Journal of Earth Sciences 30: 449-459. doi: 10.3906/yer-2009-9

Işık V (2009). Ductile shear zone in granitoid of Central Anatolian Crystalline Complex, Turkey: Implications for Late Cretaceous extensional deformation. Journal of Asian Earth Sciences 34: 507–521.

Kandilli Observatory and Earthquake Research Institute, Boğaziçi University (1971). Boğazici University Kandilli Observatory and Earthquake Research Institute [Data set]. International Federation of Digital Seismograph Networks. doi: 10.7914/SN/KO

King RW, Bock Y (2000). Documentation for the GAMIT GPS Analysis Software, Program Manuel, MIT, Cambridge.

Koçyiğit A, Beyhan A (1998). A new intracontinental transcurrent structure: the Central Anatolian Fault Zone, Turkey. Tectonophysics 284: 317-336.

Koçyiğit A, Erol O (2001). A tectonic escape structure: Erciyes pull-apart basin, Kayseri, Central Anatolia, Turkey. Geodinamica Acta 14: 1-13.

Koçyiğit A, Özacar AA (2003). Extensional neotectonic regime through the NE edge of the outer Isparta angle, SW Turkey: new field and seismic data. Turkish Journal of Earth Sciences 12 (1): 67-90.

Koçyiğit A (2000). Orta Anadolu'nun genel neotektonik özellikleri ve depremselliği. Haymana-Tuzgölü-Ulukışla basenlerinin uygulamalı çalışması Bildiri Özetleri, TPJD Bülteni, Özel sayı 5: 1-26, Aksaray (in Turkish).

Koçyiğit A (2003). General neotectonic characteristics and seismicity of central Anatolia. Turkish Association of Petroleum Geologist Special Publication 5: 1-26.

Koçyiğit A (2005). The Denizli graben-horst system and the eastern limit of western Anatolian continental extension: basin fill, structure, deformational mode, throw amount and episodic evolutionary history, SW Turkey. Geodinamica Acta 18 (3–4): 167–208.

Kürçer A, Gökten E (2012). Paleoseismological three dimensional virtual photography method; a case study: Bağlarkayası-2010 trench, Tuz Gölü fault zone, Central Anatolia, Turkey. Tectonics Recent Advances, InTech 201-228.

Kürçer A, Gökten YE (2014a). Neotectonic-Period Characteristics, Seismicity, Geometry and Segmentation of The Tuz Gölü Fault Zone. Maden Tetkik ve Arama Dergisi 149 (149): 19-68.

Kürçer A, Gökten YE (2014b). Paleosismolojik üç boyutlu sanal fotoğraflama yöntemi, örnek çalışma: Duru-2011 Hendeği, Tuz Gölü Fay Zonu, Orta Anadolu, Türkiye. Türkiye Jeoloji Bülteni 57 (1): 45-72.

Kürçer A (2012). Tuz Gölü Fay Zonu'nun neotektonik özellikleri ve paleosismolojisi, Orta Anadolu, Türkiye. PhD, Ankara Üniversitesi, Fen Bilimleri Enstitüsü, Ankara, Turkey, (in Turkish).

Kürçer A, Yeleser L, Karzaoğlu H, Izladı E, Aykac S et al. (2012). Neotectonic Characteristics and paleoseismology of salt lake fault zone, Central Anatolia, Turkey. MTA Report No, 11573, Ankara, Turkey.

Leventoğlu H (1994). Neotectonic characteristics of the central part of the Tuzgölü fault zone around Mezgit (Aksaray). MSc, ODTÜ, Fen Bilimleri Enstitüsü, Ankara, Turkey.

McClusky S, Balassanian S, Barka A, Demir C, Ergintav S et al (2000). Global positioning system constraints on plate kinematics and dynamics in the eastern mediterranean and caucasus. Journal of Geophysical Research 105: 5695-5719.

McCaffrey R (2005). Block kinematics of the Pacific–North America plate boundary in the southwestern United States from inversion of GPS, seismological, and geologic data. Journal of Geophysical Research: Solid Earth, 110 (B7). doi: 10.1029/2004JB003307

McKenzie D (1972). Active tectonics of the Mediterranean Region. Geophysical Journal of the Royal Astronomical Society 30: 109–185.

McKenzie D (1978). Active tectonics of the Alpine—Himalayan belt: the Aegean Sea and surrounding regions. Geophysical Journal International 55 (1): 217-254.

Okada Y (1985). Surface deformatıon due to shear and tensile faults in a half-space. Bulletin of the Seismological, Society of America, 75 (4): 1135-1154.

Oktar O, Erdoğan H (2018). Research of behaviors of continuous GNSS station by signal analysis methods. Earth Sciences, Research Journal 22 (1): 19- 27.

Özener H, Arpat E, Ergintav S, Doğru A, Çakmak R et al. (2010). Kinematics of the eastern part of the North Anatolian Fault Zone. Journal of Geodynamics 49: 141–150.

Özsayın E, Ciner TA, Rojay FB, Dirik RK, Melnick D et al. (2013). Plio-Quaternary extensional tectonics of the Central Anatolian Plateau: a case study from the Tuz Gölü Basin, Turkey. Turkish Journal of Earth Sciences 22 (5): 691-714.

Öztürk MZ, Şener MF, Şener M, Şahiner E (2018). Quaternary slip-rates of the Bor segment of Tuzgölü fault zone. Ömer Halisdemir Üniversitesi Mühendislik Bilimleri Dergisi 7 (3): 1049-1053 (in Turkish with English abstract).

Poyraz F, Hastaoğlu KO, Koçbulut F, Tiryakioğlu I, Tatar O et al. (2019). Determination of the block movements in the eastern section of the Gediz Graben (Turkey) from GNSS measurements. Journal of Geodynamics 123: 38-48.

Reilinger R, McClusky S, Vernant P, Lawrence S, Ergintav S et al. (2006). GPS constraints on continental deformation in the Africa-Arabia-Eurasia continental collision zone and implications for the dynamics of plate interactions. Journal of Geophysical Research 111: B05411.

Saastamoinen J (1973). Contributions to the theory of atmospheric refraction. Bulletin Géodésique 107 (1): 13-34. doi: 10.1007/bf02522083

Scherneck HG (1991). A parametrized solid earth tide model and ocean tide loading effects for global geodetic baseline measurements. Geophysical Journal International 106 (3): 677-694. doi: 10.1111/j.1365-246x.1991.tb06339.x

Simão NM, Nalbant SS, Sunbul F, Mutlu AK (2016). Central and eastern Anatolian crustal deformation rate and velocity fields derived from GPS and earthquake data. Earth and Planetary Science Letters 433: 89-98.

Springer TA, Beutler G, Rothacher M (1999). A new solar radiation pressure model for GPS satellites. GPS Solutions 2 (3): 50-62. doi: 10.1016/S0273-1177(99)00158-1

Şaroğlu F, Emre Ö, Boray A (1987). Türkiye'nin diri fayları ve depremselliği, MTA Rapor No: 8174 (in Turkish).

Şengör AMC (1980). Türkiye'nin neotektoniğinin esasları. Türkiye Jeoloji Kurumu yayını, 40 (in Turkish).

Şengör AMC, Görür N, Şaroğlu F (1985). Strike-slip faulting and related basin formation in zones of tectonic escape: Turkey as a case study. The Society of Economic Paleontologists and Mineralogists, Special Publication 37: 227-264.

Tatar O, Poyraz F, Gürsoy H, Cakir Z, Ergintav S et al. (2012). Crustal deformation and kinematics of the Eastern Part of the North Anatolian Fault Zone (Turkey) from GPS measurements. Tectonophysics 518: 55-62.

Tiryakioğlu İ (2015). Geodetic aspects of the 19 May 2011 Simav earthquake in Turkey. Geomatics, Natural Hazards and Risk, 6 (1): 76-89.

Tiryakioğlu İ, Floyd M, Erdoğan S, Gülal E, Ergintav S et al. (2013). GPS constraints on active deformation in the Isparta angle region of SW Turkey. Geophysical Journal International 195 (3): 1455–1463.

Tiryakioğlu İ, Yiğit CÖ, Yavaşoğlu H, Saka MH, Alkan RM (2017). The determination of interseismic, coseismic and postseismic deformations caused by the Gökçeada Samothraki earthquake (2014, Mw: 6.9) based on GPS data. Journal of African Earth Sciences 133: 86–94.

Tiryakioglu İ, Gulal E, Solak HI, Ozkaymak C (2018a). Crustal Deformation Modelling by GNSS Measurements: Southwestern Anatolia, Turkey. In: Kallel A, Ksibi M, Ben Dhia H, Khélifi N (eds) Recent Advances in Environmental Science from the Euro-Mediterranean and Surrounding Regions. EMCEI 2017. Advances in Science, Technology & Innovation (IEREK Interdisciplinary Series for Sustainable Development). Springer, Cham doi: 10.1007/978-3-319-70548-4_547

Tiryakioğlu I, Özkaymak Ç, Baybura T, Sözbilir H, Uysal M (2018b). Comparison of Palaeostress Analysis, Geodetic Strain Rates and Seismic Data in the the Western Part of the Sultandağı Fault in Turkey. Annals of Geophysics 61 (3). doi: 10.4401/ag-7591

Toprak V, Göncüoğlu MC (1993). Tectonic control on the development of the Neogene-Quaternary Central Anatolian Volcanic Province, Turkey. Geological Journal 28 (3-4): 357-369.

Toprak V (2000). Tuzgölü Fay Kuşağı Hasandağ Kesiminin Özellikleri, Haymana-Tuzgölü-Ulukışla Basenleri Uygulamalı Çalışma 9-11 Ekim 2000. Türkiye Petrol Jeologları Derneği Özel sayı 5: 71-84 (in Turkish).

Uygun A (1981). Tuzgölü havzasının jeolojisi, evaporit oluşumları ve hidrokarbon olanakları. TJK İç Anadolu'nun Jeolojisi Sempozyumu, Ankara, 66-71 (in Turkish).

Uygun A, Yaşar M, Erkan MC, Baş H, Çelik E et al. (1982). Tuzgölü Havzası projesi. Cilt 2, MTA Raporu (in Turkish).

Uzel T, Eren, K, Gulal E, Tiryakioğlu İ, Dindar AA et al. (2013). Monitoring the tectonic plate movements in Turkey based on the national continuous GNSS network. Arabian Journal of Geosciences 6: 3573–3580. doi: 10.1007/s12517-012-0631-5

Wells DL, Coppersmith KJ (1994). New empirical relationships among magnitude, rupture length, rupture width, rupture area, and surface displacement. Bulletin of the Seismological Society of America 84 (4): 974-1002.

Yavaşoglu HH, Tiryakioglu I, Karabulut MF, Eyubagil EE, Ozkan A et al (2021). New geodetic constraints to reveal seismic potential of central Marmara region. Turkey. Bulletin of Geophysics and Oceanography 62 (3): 513-526.

Yavaşoğlu HH, Tarı E, Tüysüz O, Çakır Z, Ergintav S (2011). Determining and modeling tectonic movements along the central part of the North Anatolian Fault (Turkey) using geodetic measurements. Journal of Geodynamics 51 (5): 339-343.

Yıldırım C (2014). Relative tectonic activity assessment of the Tuz Gölü fault zone; Central Anatolia, Turkey. Tectonophysics 630: 183-192.